15th IMEKO TC10 Workshop on Technical Diagnostics
Technical Diagnostics in Cyber-Physical Era
Budapest, Hungary, June 6-7, 2017

On-component multilayer tri-axial capacitive probe for clearance measurement

Tommaso Addabbo[1], Francesco Bertocci, Ada Fort[1], Marco Mugnaini[1], Valerio Vignoli[1], Chiara Cinelli[2]

[1] Department of Information Engineering and Mathematical Science, University of Siena, via Roma 56, 53100 Siena, Italy, ada.fort@unisi.it
[2] Nuovo Pignone Tecnologie SRL, via Felice Matteucci 2, 50127 Firenze, Italy, chiara.cinelli@ge.com

Abstract – In this paper, an on-component triaxial capacitive probe for clearance measurement (static and dynamic measurement of distance) is proposed and studied. The device is designed to be deposited onto machinery components or complex structures and is aimed at reducing the impact of probe mounting on the monitored component. The problem is discussed from a theoretical point a view and then supported by the development of a prototype in screen printed technology. The results prove the feasibility of this innovative device.

I. INTRODUCTION

'On-component' sensors, printed or deposited onto machine components have many obvious advantages: a negligible mass, accurate placement, applicability to a variety of materials including ceramics, capability for operation to very high temperatures (>1000 °C), minimal structural disturbance (minimal machining) and finally an intimate sensor to substrate contact. The use of such sensors, instead of traditional 'bulk' devices, allows for preserving the integrity of the components, not perturbing the operating conditions and the operation of the whole system, and accordingly permitting to ensure greater reliability. Some solutions based on the deposition of thin films have been since a long time the subject of study in the field of avionics. In this context, NASA has produced prototypes of sensing films for the measurement of temperature and flow sensors based on thermocouples and resistive strain gauges [1-6]. In different studies reported in the literature materials and deposition techniques suitable for particularly hostile operating conditions have been identified, especially in terms of temperature (up to 1100 °C). Both conductive and insulators ceramic materials for this application have been identified: the latter are able to maintain high insulation at temperatures up to 700 °C with a film thickness even less than 10 μm and can be deposited on either steel or similar alloys. The feasibility of multi-layer structures was also proven.

These results constitute a solid basis for the study and the realization of capacitive sensors deposited directly onto turbomachinery components. In particular, in this paper we explore the possibility of realizing triaxial capacitive probes for clearance measurement (static and dynamic measurements of distances). The structure to be achieved is quite complex, since it requires the construction of sensors consisting of a large number of layers of different materials. The problem is discussed from a theoretical point a view and then supported by the development of a prototype of a film-based triaxial capacitive sensor in screen printed technology. The proposed structure is designed, studied through electric field simulations and finally realized and tested.

II. SENSOR DESIGN AND STUDY OF THE ELECTRICAL BEHAVIOR

The proposed 'on-component' sensor has to operate as a bulk triaxial capacitive probe, whose structure is reported for sake of clarity in Fig. 1.

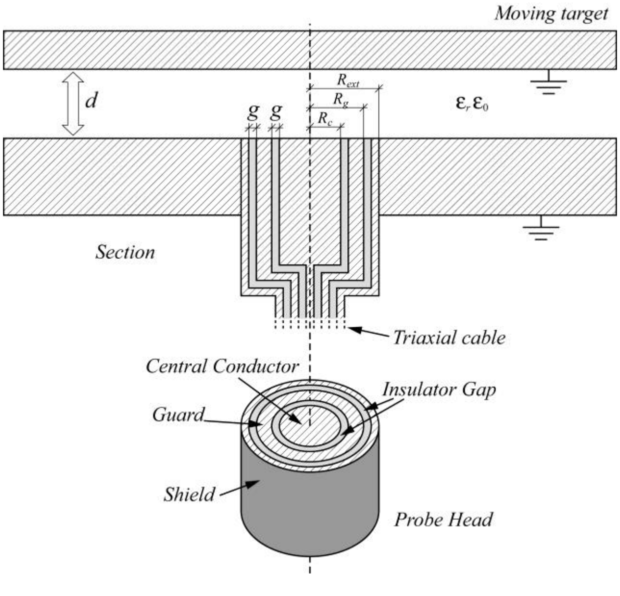

Fig. 1. structure of the traditional 'bulk' triaxial capacitive sensor.

The design of the sensor was based on the results obtained in previous studies concerning the traditional triaxial probes [7]. In particular, taking into account that the measuring electrode and the guard shield are maintained at the same voltage by the external front-end circuit, and referring to the symbols defined in Fig. 1 and Fig. 2, the sensing capacitance, CS, is given by the capacitance between the central conductor and ground:

$$C_s = C_{ct} + C_{cs} \tag{1}$$

In the literature there are several approximations for this capacitance depending, of course, on the distance from the target (that is the quantity of interest) but also on the insulating material thickness. In particular if CCS is negligible, (i.e. when the guard conductor has a large area), CS can be estimated, taking account of boundary effects due to the gap between the guard and the central (g), with the following equation [7], [8]:

$$C_s \approx C_{SO} = \frac{\varepsilon_r \varepsilon_0}{d} \pi \left(R_C + \frac{g}{2} \right)^2 \tag{2}$$

In Eq. (2) the relationship between capacitance and distance is described by the parallel plate capacitance approximation, therefore the presence of the gap does not affect in any way the behavior of the sensor, but by increasing its sensitivity. According to this model there will be no error if the measurement system uses the approximation of parallel plate to determine the distance. It is apparent that in this approximation the effect of variable distance between the electrode and the target is not accounted for, but this dependency definitely exists. Nevertheless it was shown in [7] that this simple model describes satisfactorily the behavior of the sensor, if the ratio of the outer radius of the guard and the maximum distance to the target is large ($2d \leq R_c + g$).

The layout of the proposed printed sensor is shown in Figure 3 and consists of:

a) the measurement electrode or central conductor;
b) the insulating layer between the measurement electrode and a guard shield (insulator gap);
c) the guard shield;
d) the insulating layer between the guard and the external shield (insulator gap);
e) the external shield.

The measurement electrode (and the signal wire) consists of the conductive layer (a). The electrode size is decided according to the required sensitivity. Note that the realization of printed devices allows the use of larger electrodes with respect to the traditional probes because the mounting of a probe with a large area does not affect the functionality and the integrity of the machine.

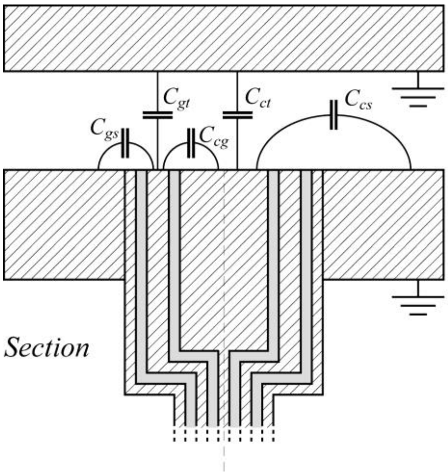

Fig.2. Definition of the equivalent capacitances for the triaxial probe

The insulating layer between the central electrode and the guard shield must completely cover the connection and is therefore realized with two depositions of ceramic or glass (b). Even the guard shield must completely cover the signal wire, and must therefore be realized through the two metal or conductive depositions indicated by (c) in Figure 3. The two layers indicated with (d) insulate the guard from the external shield. Note that in the prototype an alumina support acts as the outer insulating layer. The external shield (e) must constitute a closed conductive structure realized by two further outer conductive layers. In the final device, the metal component that supports the sensor acts as the lower part of the external shield.

Note that electrodes with different geometry (e.g. rectangles) can be realized without drawbacks. The geometry chosen and realized by a prototype is similar to that of the traditional probe, this choice has been made to facilitate the comparison of performance with traditional probes.

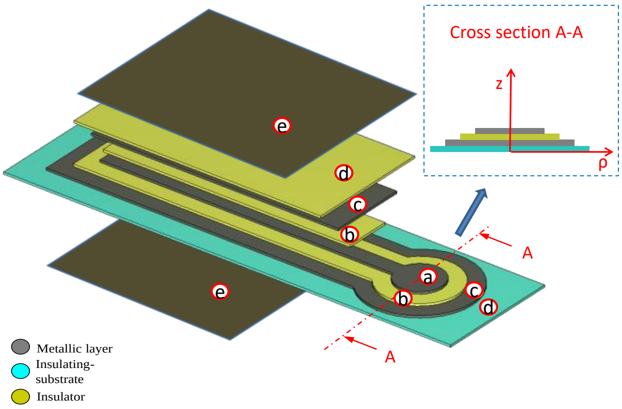

Fig. 3. Structure of the printed sensor, and reference system for the following figures.

Obviously, the printed probe has the advantage, compared to traditional probe, not to have a gap between the central and the guard electrode.

The proposed probe was studied by finite element analysis (FEA) of the electric field. To perform these simulations we refer to the application of interest, in which the measurement range is centered at 500 μm (extendable up to 4 mm), and the required accuracy is of the order of 10 μm (at 500 μm).

In the general case, the results of the FEA simulations show that the electric field generated by a sensor with the geometry shown in Fig. 3 is disturbed, if compared to the ideal situation of a uniform field generated by a capacitor with infinite parallel plane plates, firstly due to the presence a height difference between the central electrode and the guard, whereas the fringe effect due to the finite area of the guard is completely irrelevant if the guard is sufficiently large (compared to the maximum distance to be measured).

Figure 4 highlights the effect of the guard-central electrode difference in height. In the figure the results are obtained considering an overall height difference between measurement electrode and guard surfaces of 100 μm. The simulation concerns a sensor in which the central electrode (a) and the insulation layer (b) have the same radius. As expected, in this case, the edge effect is rather large and its influence is linked to the distance to be measured.

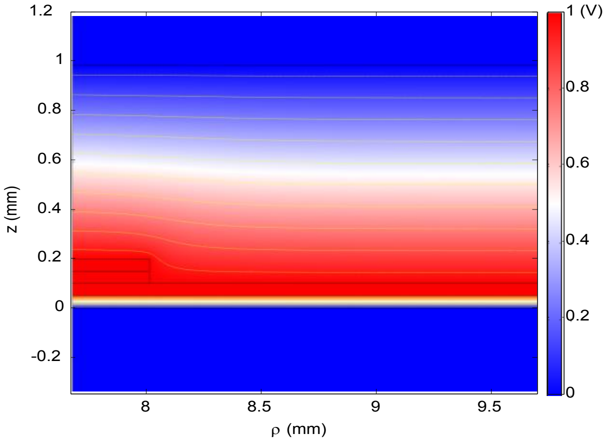

Fig. 4. Electrical field FEA. The figure shows the voltage in false color, the equipotential lines are also shown. The voltage target-sensor is equal to 1V, the distance from the guard to the target is $d = 0.9$ mm. The guard radius is $2R_c$. The insulating layer has a relative dielectric constant equal to 11 and a radius equal to R_c., $t_{DIE} = t_c = 50\ \mu m$.

The fringe effect can be described roughly by the transition from the electrical field $E_g \approx V / d$ (above the center of the guard ring far from the electrode edge) to the one given by $E_c \approx V / (d - t_{DIE} - t_c)$ (above the center of the measurement electrode), where t_{DIE} is the thickness of the layer insulating the guard from the central electrode whereas t_c is the thickness of the electrode itself, and d is the distance between target and guard.

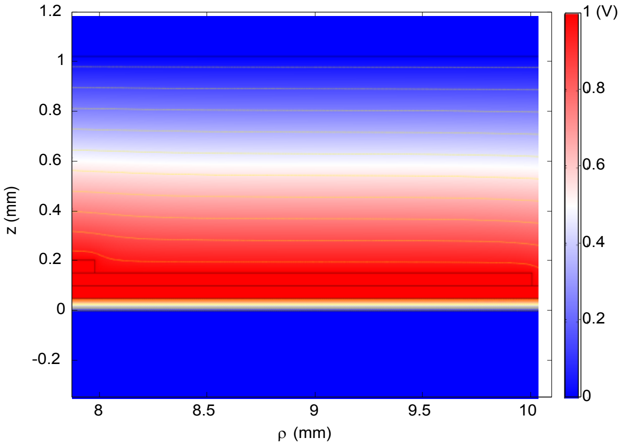

Fig. 5. Electrical field FEA. The figure shows the voltage in false color, the equipotential lines are also shown. The voltage target-sensor is equal to 1V, the distance from the guard to the target is $d = 0.9$ mm. The guard radius is $2R_c$. The insulating layer has a dielectric constant equal to 11 and has a radius equal to $R_c + 2$ mm, $t_{DIE} = t_c = 50\mu m$.

Using a fixed value for the thicknesses of the dielectric and the central electrode, as can be seen in Figs. 4 and 5, the edge effect can be minimized if the insulation is realized by a material with a large dielectric constant and if the insulating layer area is increased.

In fact, with reference to Fig. 5, using the approximation of infinite parallel plates to describe the field and the electric potential over the guard ring, far from the sensor central electrode, it is possible to write:

$$V_g(z) = V - \frac{V}{t_{DIE} + \varepsilon_r (d - t_{DIE})} z \qquad 0 < z < t_{DIE}$$

$$\begin{aligned} V_g(z) = V - \frac{V}{t_{DIE} + \varepsilon_r (d - t_{DIE})} t_{DIE} + \\ - \frac{\varepsilon_r V}{t_{DIE} + \varepsilon_r (d - t_{DIE})} (z - t_{DIE}) \qquad t_{DIE} < z < d \end{aligned} \tag{3}$$

Therefore realizing the insulating layer between the central electrode and the guard with a radius larger than R_c and choosing a material which has a large dielectric constant, it is possible to reduce the discontinuity between the electric field above the measurement electrode (E_c) and the one above the guard (E_g).

In fact if $\varepsilon_r >> 1$ then $V_g(t_{DIE}) \approx V$ and, for $z > t_{DIE}$, $V_g(z) \approx V - V(z-t_{DIE}) / (d - t_{DIE})$. In this case, therefore, you switch from a field $E_g \approx V / (d - t_{DIE})$ above the guard electrode to the field $E_c \approx V / (d - t_{DIE} - t_c)$ above the measuring electrode. Compared to the case in which the dielectric is located just under the central electrode, the geometry shown in Fig. 5 reduces the fringe effect related to the thickness of the insulating layer. Note that this thickness can't be too small, in order to grant a sufficient insulation between the conductive layers, whereas the metallic layer thicknesses can be very small without affecting the sensor operation, not being critical the perfect continuity.

The effect of the thickness of the measurement electrode may be further reduced by depositing another dielectric layer.

The geometry shown in Fig. 5 allows for treating the printed probe as a 'traditional' bulk triaxial probe with the same size, with a measuring capacitance given by Eq. (2), being $g=0$.

III. EXPERIMENTAL RESULTS

A prototype with the structure shown in Fig. 3 was developed on an alumina substrate in screen printing technique. The measurement electrode radius is 4.5 mm, whereas its thickness is 12 μm. The insulating layer (Resistivity >100 GΩ cm @25 °C) between the guard and the measurement electrode has a radius of 6.5 mm and thickness of 50 μm (Fig. 6).

Fig. 6. Prototype after having deposited the first three layers.

The proposed device will be used to perform both static and dynamic measurements of distance. To test the device in a large frequency range, an automatic measurement system was developed. The system provides an accurate capacitance-voltage conversion in the bandwidth 10 Hz – 10 kHz. The measurement system provides both an analysis of the frequency behavior of the device (influence of parasitic components) and a calibration of the sensor with respect to distance. The test system is shown in Fig. 7.

The sensor under test is placed at a known distance d (accuracy 0.3 mm) from a metallic plate, which is driven by a waveform generator (Agilent AG33220A), at the known voltage $V_{in}(t)$ with respect to the ground. The charge, $Q(t)$, induced on the measuring electrode is converted into a voltage by a charge amplifier (Bruel and Kjaer Nexus 2692-A).

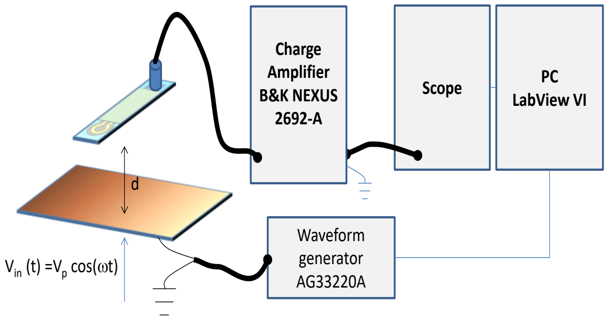

Fig. 7 test system

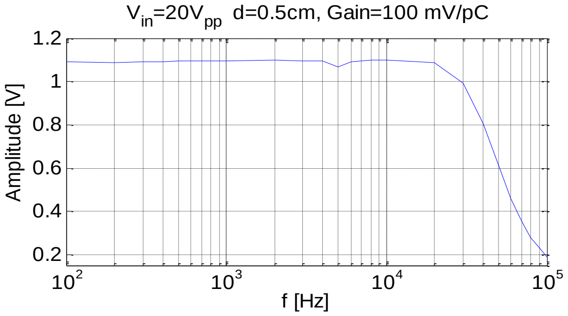

Fig.8. Measured $V_{out}(t)$.

The guard and the shield are connected to the voltage reference of the charge amplifier. The expected charge is given by the following:

$$Q(f)=V_{in}(f)C_s=\frac{V_{in}(f)\varepsilon\pi R_c^2}{d}, \qquad (4)$$

where R_c for the prototype is 4.5 mm. The output of the charge amplifier, $V_{out}(t)$, is given by:

$$V_{out}(f)=Q(f)H(f), \qquad (5)$$

where $H(f)$ is the transfer function of the charge amplifier (bandwidth-10% 1 Hz to 30 kHz). At the frequency f_0 in the center of the frequency band the distance d can be assessed exploiting the above equations:

$$d_{measured}=\frac{|V_{in}(f_0)|}{|V_{out}(f_0)|}\varepsilon\pi R_c^2 \qquad (6)$$

The expected accuracy due to accuracy of the voltage measurements and to the tolerance given by the printing process is of 5%. The results of such an estimation, reported in Fig. 9 confirm that the behavior of the printed probe is the one expected. The behavior of the proposed probe was compared to a the one of a traditional triaxial probe with the same size, showing similar performance also in term of noise.

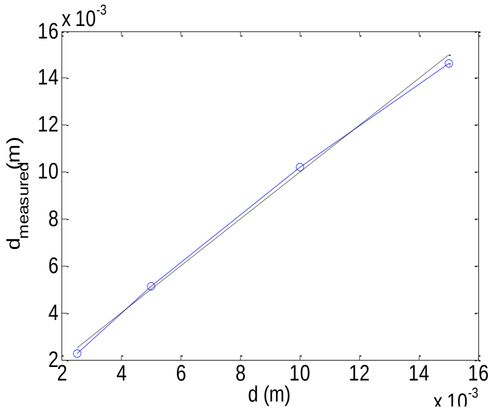

Fig. 9. Experimental results

IV. CONCLUSION

The feasibility of an ‘on-component’ triaxial capacitive probe for clearance monitoring is demonstrated both from a theoretical and an experimental point of view. In particular, the test of a prototype in screen printed technology demonstrated that the behavior of such components is comparable with the one of a ‘bulk’ triaxal probe. The next step of this work will be to deposit and test a similar structure on turbomachinery components.

REFERENCES

[1] R.D. Meredith, J.D. Wrbanek, G.C. Fralick, L.C. Greer, G.W. Hunter, L.Y. Chen, “Design and operation of a fast, thin-film thermocouple probe on a turbine engine”, 50th AIAA/ASME/SAE/ASEE Joint Propulsion Conference, 2014.

[2] A. Von Moll, A.R. Behbahani, G.C. Fralick, J.D. Wrbanek, G.W. Hunter, “A Review of exhaust gas temperature sensing techniques for modern turbine engine controls”, 50th AIAA/ASME/SAE/ASEE Joint Propulsion Conference, 2014, 18.

[3] J.D. Wrbanek, G.C. Fralick, D. Zhu, “Ceramic thin film thermocouples for SiC-based ceramic matrix composites”, Thin Solid Films, 520 (17), 2012, pp. 5801-5806.

[4] J.D. Wrbanek, G.C. Fralick, “Thin film ceramic strain sensor development for harsh environments”, Proceedings of the 53rd International Instrumentation Symposium, 2007, vol. 470, pp. 551-572.

[5] O.J. Gregory, E. Busch, G.C. Fralick, “Thermoelectric properties of ceramic thin film thermocouples”, Proceedings of the 52nd International Instrumentation Symposium, 2006, vol. 467, pp. 234-248.

[6] J.D. Wrbanek, G.C. Fralick, J.M. Gonzalez III, “Developing multilayer thin film strain sensors with high thermal stability”, Collection of Technical Papers - AIAA/ASME/SAE/ASEE 42nd Joint Propulsion Conference, 2006, vol. 4, pp. 2731-2740.

[7] T. Addabbo, A. Fort, M. Mugnaini, S. Rocchi, V. Vignoli, “A heuristic reliable model for guarded capacitive sensors to measure displacements”, Proceedings of the 2015 IEEE International Instrumentation and Measurement Technology Conference (I2MTC), Pisa, 2015, pp. 1488-1491.

[8] T. Addabbo, A. Fort, M. Mugnaini, S. Rocchi, V. Vignoli, “Improved model for the capacitance estimation of guarded capacitive sensors”, Proceedings of the 2015 XVIII AISEM Annual Conference, Trento, 2015, pp. 1-4.